

# New technique for the reduction of helicity-correlated instrumental asymmetries in photoemitted beams of spin-polarized electrons

J. M. Dreiling,\* S. J. Burtwistle, and T. J. Gay

Jorgensen Hall, University of Nebraska, Lincoln, Nebraska 68588-0299, USA

\*Corresponding author: jmdreiling2@gmail.com

Received 1 October 2014; accepted 11 December 2014;  
posted 16 December 2014 (Doc. ID 223957); published 26 January 2015

We present a new optical system that significantly reduces helicity-dependent instrumental intensity asymmetries. It is an extension of a previous scheme [Appl. Opt. **47**, 2465 (2008)], where one laser beam is split using a polarizing beam splitter into two with orthogonal linear polarizations. The beams are sent through a chopper, allowing only one to pass at a time. The two temporally separated beams are then spatially recombined using a second beam splitter. A liquid crystal retarder preceding the first beam splitter controls the relative intensity of the two oppositely polarized beams, allowing reduction of instrumental asymmetries. This system has been modified to include a spatial filter and a Pockels cell placed after the second beam splitter to act as a second active polarization element. Using this method, we can control instrumental asymmetries to  $\sim 5 \times 10^{-7}$  in 1 h of data taking, which is comparable to the precision achieved in “second-generation” high energy electron-nuclear scattering parity violation experiments. © 2015 Optical Society of America

*OCIS codes:* (080.2740) Geometric optical design; (120.4570) Optical design of instruments; (120.4820) Optical systems; (220.1080) Active or adaptive optics; (220.2740) Geometric optical design; (220.4830) Systems design.

<http://dx.doi.org/10.1364/AO.54.000763>

## 1. Introduction

Beams of spin-polarized electrons [1] are used in, e.g., high-energy nuclear physics to study parity violation [2–4], in condensed matter physics to study the morphology of magnetic domains [5], and in molecular physics to study chiral sensitivity in electron-molecule collisions [6–8]. The standard method used to produce polarized electrons is laser-induced photoemission from a negative electron affinity (NEA) GaAs crystal [9]. This method has the advantage that the electron spin can be flipped by optical means, so that first-order instrumental spin-dependent asymmetries can be eliminated by simply reversing the circular polarization of the

laser beam [10]. Unfortunately, such asymmetries may persist to higher order and may also drift in time. Optical elements that reverse the laser beam’s helicity invariably, at some level, cause it to have spatial and/or intensity variations that are correlated with this reversal. Such instrumental asymmetries generally result in spin-dependent variations in the photo-emitted electron beam which mimic the experimental asymmetry. These problems can be particularly pernicious when the experimental asymmetries to be measured are very small, such as those in the most recent generation of nuclear parity violation experiments, which are of the order of  $10^{-8}$  [3].

In this paper, we define the “source instrumental intensity asymmetry” of a polarized electron source or of the current coming from a photo-diode as

$$A_S = \frac{I^R - I^L}{I^R + I^L}, \quad (1)$$

where  $I^{R(L)}$  is the current corresponding to the right (left)-handed circularly-polarized laser light producing that current. For an ideal system,  $A_S = 0$ . We are currently conducting experiments to measure spin-dependent asymmetries when a beam of longitudinally-polarized electrons, produced by a GaAs photocathode source, is passed through a vapor of chiral molecules (see Fig. 1) [8,9,11]. After the electron beam leaves the photocathode, it must travel nearly a meter through the apparatus before interacting with a target. As a result of the long path length, small values of  $A_S$  at the source, caused by helicity-dependent laser intensity or position variations, can be magnified significantly when the beam reaches the target.

In what follows, we will be careful to distinguish between  $A_S$  and the “target instrumental intensity asymmetry,”  $A_T$ , which is measured on the Faraday cup at the opposite end of the apparatus. It is important to note that in our experiment, the actual values of  $A_S$  or  $A_T$  are relatively unimportant. As long as they are constant, they can be measured and subtracted from any “physics” asymmetry. However, variations over time in these quantities can cause serious problems because such drifting cannot be assessed during the course of data runs with the chiral target in place. Generally, the variation of  $A_T$  is greater than that of  $A_S$  and is more important because it can lead directly to measurements of false “physics” asymmetries, producing nonzero values even for achiral targets. The values of  $A_S$  measured with a photodiode are essentially just a measure of the instrumental asymmetry of the optical system alone. With the current apparatus, if  $A_S$  is being measured with a photodiode, it is the only asymmetry that can be monitored as the photodiode blocks the laser from the photocathode. In the actual experiment, we monitor the GaAs photocathode current to construct  $A_S$ , minimize it and keep it

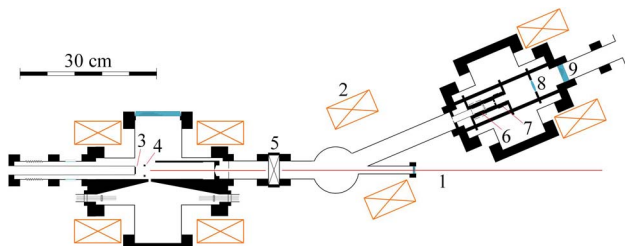


Fig. 1. Polarized electron source and target chamber. (1) laser beam from active feedback optical system for the GaAs source; (2) solenoidal guiding magnets; (3) GaAs photocathode; (4) NEA activation cesiators; (5) gate valve; (6) chiral target cell; (7) optical polarimeter target cell; (8) fluorescence collection lens; (9) window for the optical polarimeter. Instrumental current asymmetries  $A_S$  and  $A_T$  are measured using the photoemission current from the GaAs photocathode (3) and the current detected on the Faraday cup immediately following the target cell (6), respectively.

nearly constant with feedback control, and then use measurements of  $A_T$  to set the experimental asymmetry “zero.”

In 2008, our group employed an active-feedback scheme to control the standard deviation of the mean (SDM) of  $A_S$  as measured by a photodiode to  $2 \times 10^{-6}$  [12]. That work was based on a simple feedback scheme that relied on the digitized response of the photodiode to the laser beam whose helicity was flipped by a combination of chopper and beam-splitting cubes. Importantly, the feedback element that was controlled was not actively used to flip the laser’s helicity. In this report, we discuss an improvement of that method that employs a Pockels cell as a secondary helicity flipper and a spatial filter to improve the system’s alignment. This has yielded photodiode  $A_S$  SDM values almost two orders of magnitude smaller:  $3 \times 10^{-8}$ . The new apparatus can provide control of  $A_T$  to yield a SDM better than  $5 \times 10^{-7}$  in 60 min of data acquisition.

## 2. Apparatus

The new optical train is shown in Fig. 2 [11]. Linearly polarized light from a Sacher Lasertechnik 780 nm laser (Cheetah, laserhead TEC 50) is directed through a half-wave plate to rotate the plane of linear polarization. It then passes through a Meadowlark LVR-200 liquid crystal retarder (LCR) and a polarizing beam splitter (Thorlabs PBS253). The two beams emerging from the polarizing beam splitter are orthogonally linearly-polarized and are sent through a mechanical chopper wheel (SRS 540) on parallel paths. The chopper wheel is oriented so that only one beam is allowed to pass through it at a time. The two beams are then spatially recombined using a second polarizing beam splitter, and the recombined beam passes through a spatial filter

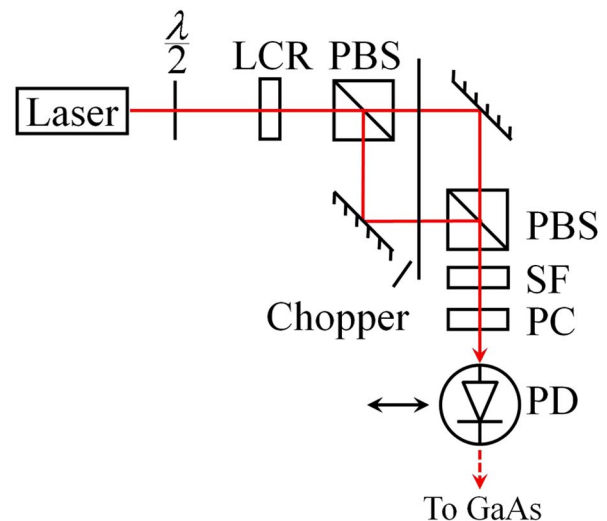


Fig. 2. The optical setup. Elements used include LCR—liquid crystal retarder, PBS—polarizing beam splitter, SF—spatial filter, PC—Pockels cell, and PD—photodiode. The photodiode is moved in and out of the path of the laser beam. When it is in the path, the laser is blocked from hitting the GaAs photocathode.

(Newport five-axis model 910). The spatial filter itself is gimballed and consists of an initial alignment aperture, a lens, and translatable pin-hole aperture. A Pockels cell (Conoptics M350-50) circularly polarizes the final beam with alternate helicities before it enters the electron beam apparatus through a nondichroic window (Fig. 1).

We discuss the asymmetries that were measured using three different signals: the current from a photodiode (Thorlabs DET110) just upstream of the entrance window ( $A_S$ ), the current drawn from the photocathode (also  $A_S$ , but with the photodiode removed from the laser beam path), and the current measured on the Faraday cup assembly in the target cell ( $A_T$ ). In the latter two cases, the currents were transmitted through short BNC cables connected to Stanford Research Systems SR570 low-noise current preamplifiers whose outputs were sent to SR830 DSP lock-in amplifiers (Fig. 3); the photodiode output was sent directly to a lock-in amplifier. For the photodiode or photocathode, the lock-in is designated as the “control” lock-in, while a second “monitor” lock-in is used for the Faraday cup signal. The lock-ins are set such that their output is proportional to the asymmetry  $A_S$  or  $A_T$ ; the control lock-in provides  $A_S$ , while the monitor lock-in detects  $A_T$ . Usually, the lock-ins are referenced to the chopper wheel frequency. The exception to this is the final optical configuration combining the two-beam system and the Pockels cell (discussed in more detail later), in which case the monitor lock-in is set to detect the component at twice the chopper frequency.

To achieve a stable  $A_S$ , the control lock-in output is sent to a SRS SIM960 analog proportional-integral-derivative (PID) controller (Fig. 3). The PID controller’s operation is centered upon the error signal,  $\varepsilon$ ,

calculated as the difference of the measured value ( $\tilde{M}$ ) and the setpoint value ( $\tilde{S}$ ):

$$\varepsilon = \tilde{S} - \tilde{M}. \quad (2)$$

The output of the PID controller is based upon the result of passing the error signal through three channels:

- (1) The proportional path with gain  $P$ ;
- (2) The integral path with gain  $I$ ;
- (3) The derivative path with gain  $D$ .

The values of  $P$ ,  $I$ , and  $D$  are each individually set by the user. Additionally, a constant offset ( $\tilde{V}_o$ ) can be programmed. The output ( $\tilde{V}$ ) is then given by

$$\tilde{V} = P\left(\varepsilon + I \int \varepsilon dt + D \frac{d\varepsilon}{dt}\right) + \tilde{V}_o. \quad (3)$$

This output signal determines the voltage applied to the LCR and thus its retardance, thereby enabling active feedback to reduce and stabilize  $A_S$ . The value of  $A_T$  corresponding to the Faraday cup current is thus passively controlled. With this setup, it is easier to feedback when  $A_S$  is small and nonzero. As long as it is constant, however, any resultant nonzero value of  $A_T$  can be subtracted from an experimental “physics” asymmetry, as previously mentioned. This optical arrangement (as well as our earlier one [12]) solves the problem of using an electro-optic element—which will invariably produce spatial variations—as both the active feedback and the helicity-flipping component.

This setup includes the following improvements over our previous setup.

(1) A more stable laser. The light source used for photoemission from the GaAs photocathode was chosen based on power and laser-pointing stability over time. Initially, we used a temperature-stabilized Power Technology Incorporated diode laser (Model LDCU5/7873) with 75 mW of power, but later we switched to the Sacher Lasertechnik unit due its increased stability. The Sacher laser has a maximum of  $\sim 70$  mW output power.

(2) A better chopper mounting and alignment. The chopper wheel plays a crucial role in the experiment and requires a great deal of attention to detail in its operation. We ultimately decided to use a wheel with six slots and a chopper frequency of  $\sim 210$  Hz [11]. Using frequencies close to 60 Hz or multiples thereof should be avoided to minimize line noise.

The edges of the chopper blades can affect the asymmetry signal if the beams are slightly misaligned. The chopper wheel positioning must be adjusted to minimize these transient features in the intensity profile of the recombined beam that result from the chopper blade passing through the laser beam profile. Such features add unwanted Fourier components to the asymmetry signal, so the wheel is adjusted to minimize their effect.

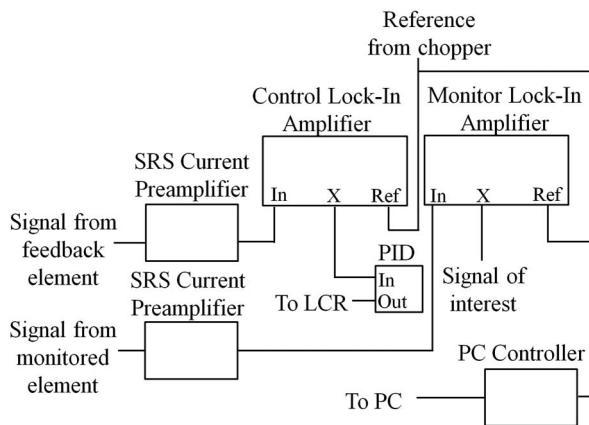


Fig. 3. Block diagram of the electronics used in the new feedback system that combines the chopper setup with the Pockels cell (PC). The control lock-in is referenced at the chopper frequency, while the monitor lock-in is referenced at twice the chopper frequency by setting it to detect the second harmonic. The reference signal from the chopper is used to supply the trigger for the PC controller. When the optical setup does not include the PC, the electronics used are the same, with the exception that the PC and its controller are removed. In these cases, both the control and the monitor lock-ins are referenced at the chopper frequency.

First, it is important to properly align the chopper wheel and the two linearly polarized laser beams. The laser alignment should be such that the two beams passing through the chopper wheel are horizontally separated by a distance just smaller than twice the outer radius of the blades themselves. The wheel in turn should be oriented so that the laser beams are roughly equally spaced horizontally relative to its center and at approximately its vertical midpoint. The chopper wheel was mounted to allow micrometer adjustments in both horizontal and vertical directions.

(3) Better laser alignment, including the use of a spatial filter. One of the key factors in minimizing instrumental asymmetries and their drifting over time is to make the two oppositely-polarized laser beams be as collinear as possible. Differences in their alignment or their intensity distributions are transferred to the electron beams of opposite polarization. As the electrons in turn propagate down the machine to the target chamber, the differences can be amplified significantly.

After initial alignment and before each data run, a meticulous laser alignment was performed with the chopper turned off using an On-Trak Photonics (PSM2-10 with controller OT-301) position-sensitive photodiode. The spatial filter helped greatly in cleaning up small misalignments and differences in intensity profiles between the two beams. This significantly reduced values of  $A_T$  and temporal variations thereof. However, using the spatial filter had the disadvantage that it reduced the power of the laser by approximately an order of magnitude, with subsequent reduction of the polarized electron beam current.

Our optical setup included a long focal-length lens to provide point-to-point focusing of the laser beam onto the crystal. This also helped with stabilization and reduction of  $A_T$ .

(4) An improved feedback system, including lock-in amplifiers and a PID controller. As mentioned above, the “control” lock-in amplifier measures  $A_S$  which is fed back on and controlled to reduce  $A_T$ , as measured by the “monitor” lock-in amplifier. The signal detected by a lock-in amplifier is  $1/\sqrt{2}$  times the magnitude of the first Fourier component value of the input signal at the reference frequency. For our system, the asymmetry input signal is approximately a square wave of amplitude  $a$  (first Fourier component  $4a/\pi$ ), where

$$a = \frac{V(I^R) - V(I^L)}{2}. \quad (4)$$

Here,  $V(I^R)$  and  $V(I^L)$  correspond to the preamplifier voltages associated with the currents for the right- and left-circularly polarized light, respectively. The signal measured by the lock-in is

$$\alpha \equiv \frac{2\sqrt{2}a}{\pi} = \frac{\sqrt{2}[V(I^R) - V(I^L)]}{\pi}. \quad (5)$$

In order to find the asymmetry as defined by Eq. (1) from the signal detected by the lock-in, we must calculate

$$A_i = \frac{V(I^R) - V(I^L)}{V(I^R) + V(I^L)} = \frac{\pi \times \alpha}{2\sqrt{2} \times V(I_0)}, \quad (6)$$

where  $i = S$  or  $T$  and

$$V(I_0) = \frac{V(I^R) + V(I^L)}{2}. \quad (7)$$

The output,  $O$ , of an SR830 lock-in is determined by the settings of the lock-in and is related to  $\alpha$  by

$$O = \frac{\alpha \times E \times 10 \text{ Volts}}{G}, \quad (8)$$

where  $E$  is the “expand” factor, and  $G$  is the chosen sensitivity of the lock-in amplifier in volts. Therefore,  $A_i$  can be calculated from the output of the lock-in using the equation

$$A_i = \frac{\pi \times O \times G}{2\sqrt{2} \times V(I_0) \times E \times 10 \text{ Volts}}. \quad (9)$$

In order to make sure that Eq. (9) is correct, we used a function generator and power supply to create an artificial asymmetry signal with known parameters to verify it. The difference between the measured and actual asymmetry was found to be  $<5\%$ .

(5) The use of a Pockels cell as a second helicity flipper. An important cause of the persistent instrumental asymmetries we observe is the fact that two distinct laser beams are used to produce the electron beams of opposite helicity. Even with the addition of the spatial filter, these two beams will always have residual small differences in both their spatial profiles and trajectories.

A similar problem arises in Mott electron polarimetry and is largely eliminated by the optical flipping of the electron spin (or the mechanical rotation of the Mott polarimeter itself) with the subsequent construction of an asymmetry “super-ratio” (see, e.g., [10]).

The adaption of this idea to our system is accomplished as shown in Fig. 2 by replacing a fixed quarter-wave plate with a Pockels cell. With this arrangement, both the Pockels cell and the two-beam/chopper setup are used to reverse the helicity of the laser beam. The Pockels cell retardation is flipped at the same frequency as that of the chopper wheel, but with a  $90^\circ$  phase shift. This is shown schematically in Fig. 4. The combination of the two polarization-reversing elements results in light whose polarization alternates between right- and left-circular at a frequency that is twice that of the chopper frequency. Thus, the monitor lock-in amplifier must be referenced at twice the chopper frequency, as previously mentioned.

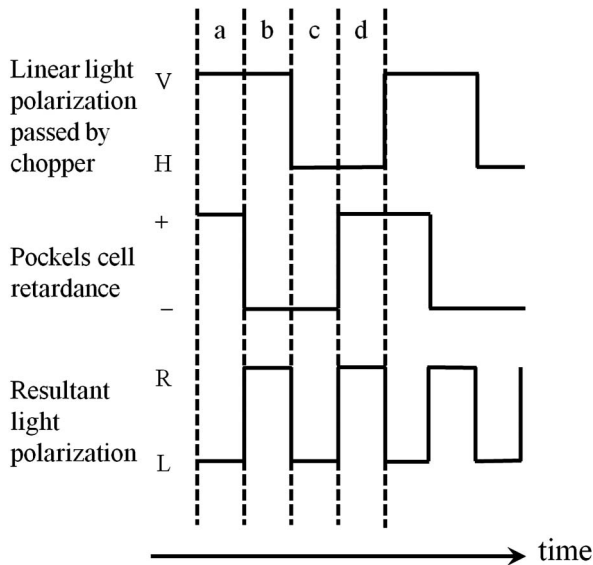


Fig. 4. Illustration of the polarization of the light produced due to the combination of the chopper and Pockels cell.

This new configuration is more effective at reducing instrumental asymmetries because both configurations of both helicity-reversing elements (chopper and Pockels cell) are used to produce both *R* and *L* light. In general, the two beams of orthogonal linear polarization passed by the chopper are slightly misaligned and/or have different distributions of intensity. Moreover, a change in the Pockels cell voltage will alter beam pointing and/or intensity distribution. Thus, for a given circular polarization of the laser beam incident on the GaAs, both chopper beam variations and Pockels cell beam steerings/intensity variations contribute to the position and intensity distribution of the laser beam on the crystal. This tends to average out instrumental asymmetries and their temporal drifting.

### 3. Procedure and Results

Instrumental asymmetry data were collected over 1 h using several different optical setups (Fig. 5). These setups varied from the most simple configuration (e.g., only one laser beam passing through a Pockels cell or the two-beam system with no additional components) to the most complex (the two-beam system with both the Pockels cell and spatial filter). The corresponding  $A_S$  or  $A_T$  values recorded over 1 h are shown in Fig. 6. The analysis of the data of Fig. 6 is summarized in Table 1. It should be noted that  $A_S$  values and their SDMs do not change appreciably when the optical setup is changed, as it is equally easy to feedback on a signal for all arrangements. However, the stability of  $A_T$  is highly dependent on the configuration used.

The maximum drift in the 60 min of data collection was calculated by taking the difference between the 2-min average value of the highest asymmetry region and the 2-min average corresponding to the lowest asymmetry. Additionally, four bins of 5-min of data were selected where the asymmetry values appeared

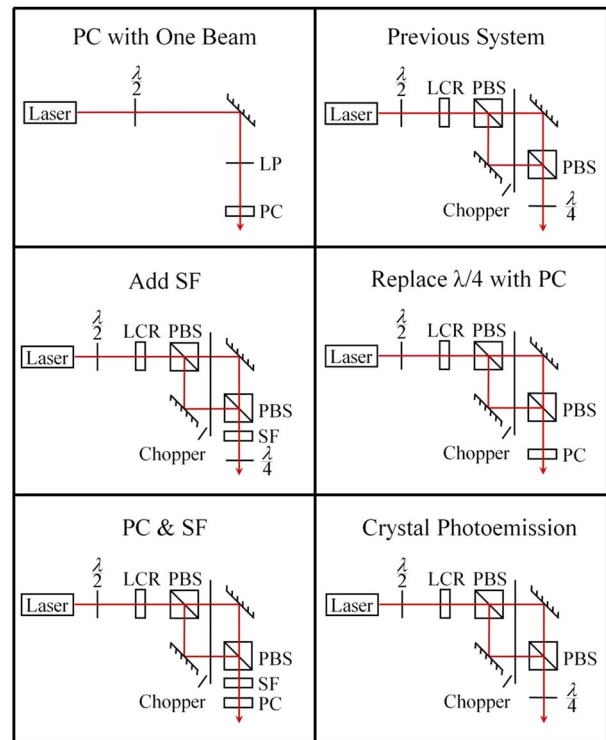


Fig. 5. Different optical setups tested. Elements used include LCR—liquid crystal retarder, PBS—polarizing beam splitter, SF—spatial filter, and PC—Pockels cell.

to be near-linear. A best-fit line for each bin was found, and those line values were subtracted from the corresponding data. Then, the standard deviation of the data in the bin was found. This was done for the four bins individually, and then an average of the four standard deviations was calculated. For the data runs where the instrumental asymmetry was essentially constant (the last three

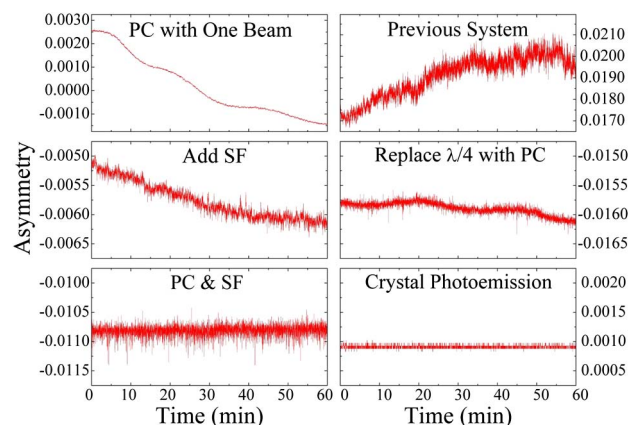


Fig. 6. Asymmetry measurements for different optical setups as shown in Fig. 5. The  $A_S$  as measured by the photoemission from the crystal (last graph) is essentially independent of the optical arrangement; it is equally easy to feedback on the signals from any of the optical configurations. However,  $A_T$  as measured at the downstream end of the apparatus on the Faraday cup (first five graphs) is highly dependent on the optical arrangement. SF—spatial filter and PC—Pockels cell.

**Table 1. Statistics for Asymmetry Variations Produced with Different Optical Setups<sup>a</sup>**

	Max. Drift in 60 Min (Max-Min)	4-Bin Standard Deviation Average	60 Min Standard Deviation of the Mean
PC with one beam	$3.97 \times 10^{-3}$	$3.61 \times 10^{-5}$	
Previous system	$2.58 \times 10^{-3}$	$7.58 \times 10^{-4}$	
Add SF	$9.60 \times 10^{-4}$	$6.12 \times 10^{-5}$	
Replace $\lambda/4$ with PC	$3.49 \times 10^{-4}$	$3.92 \times 10^{-5}$	
PC & SF	$2.54 \times 10^{-5}$	$7.88 \times 10^{-5}$	$4.56 \times 10^{-7}$
Crystal photoemission	$1.20 \times 10^{-6}$	$2.73 \times 10^{-5}$	$1.53 \times 10^{-7}$
Photodiode	$1.86 \times 10^{-6}$	$4.23 \times 10^{-6}$	$2.63 \times 10^{-8}$

<sup>a</sup>The standard deviation of the mean was taken only when drifting was minimal and was calculated for the entire 60 min of running. The stability of the feedback asymmetry ( $A_S$ ) for the photoemission from the crystal determines the limit of how stable  $A_T$  can be with the current feedback system. SF—spatial filter and PC—Pockels cell.

data sets listed in Table 1), the standard deviation of the mean (SDM) for the entire 60 min data set is also given.

The best results were produced with the combination of the Pockels cell and spatial filter. Over 1 h of data, this optical setup produced an  $A_T$  with a SDM of  $4.56 \times 10^{-7}$  as measured at the Faraday cup, which is comparable to the SDM of  $A_S$  for the photocurrent,  $1.53 \times 10^{-7}$ . Barring unusual circumstances, the SDM of  $A_S$  should be a lower limit for the SDM of  $A_T$  with the present feedback method. The fact that the SDM of  $A_T$  is approximately three times that of  $A_S$  is remarkable for this experiment; in the previous simple two-beam system, the SDM of  $A_T$  could be several orders of magnitude larger than that of  $A_S$ .

#### 4. Conclusions

We have demonstrated an optical system for the reduction of helicity-dependent instrumental asymmetries usable in polarized-electron-beam scattering experiments. Such systems find their use in experiments studying parity violation in nuclear physics and the measurement of spin-dependent cross sections in collisions between polarized electrons and atoms or molecules. Our recent experiments searching for longitudinal spin dependence in electron collisions with chiral molecules require that the electron-helicity-correlated intensity asymmetry variations associated with the electron beam incident on the target, essentially the SDM of  $A_T$ , be of order  $10^{-5}$ . We have demonstrated here SDM values of  $A_T$  in our electron scattering apparatus of  $5 \times 10^{-7}$ . In an earlier version of this optical setup, in which we only investigated a source instrumental asymmetry  $A_S$  that was measured with a photodiode and was actively controlled, we found with 1.5 h of data taking a SDM in  $A_S$  of  $2 \times 10^{-6}$ . With the new system having a more stable laser, better mechanical mounting and position control, better optical alignment, an

improved feedback system, and a second means of optical helicity reversal, the SDM of  $A_S$  was reduced almost two orders of magnitude to  $3 \times 10^{-8}$  in 1 h of running. As can be seen from Table 1, the largest part of this improvement is due to implementation of the Pockels cell.

Instrumental asymmetry control at this level is comparable to that obtained in several second-generation high-energy nuclear parity violation experiments, such as the HAPPEX series, SAMPLE, and SLAC Experiment E158 [2–4,13]. These experiments typically achieved uncertainty due to helicity-correlated beam asymmetries of the order of  $10^{-7}$ – $10^{-8}$  over days of running time, compared with our  $A_T$  SDM value of  $5 \times 10^{-7}$  obtained in 1 h.

This work was funded by the National Science Foundation through Grant No. PHY-1206067 and the NASA Nebraska Space Grant. The authors thank H. Batelaan, K. W. Trantham, E. T. Litaker, and S. D. Ducharme for useful discussions and the loan of equipment.

#### References

1. J. Kessler, *Polarized Electrons*, 2nd ed. (Springer-Verlag, 1985).
2. M. Farkhondeh, W. Franklin, E. Tsentalovich, and T. Zwart, “Helicity-correlated effects in the SAMPLE experiment,” *AIP Conf. Proc.* **675**, 1024–1028 (2003).
3. P. Mastromarino, T. B. Humensky, P. Anthony, C. Arroyo, K. Bega, A. Brachmann, G. Cates, J. Clendenin, F.-J. Decker, T. Fieguth, E. Hughes, G. M. Jones, Y. Kolomensky, K. Kumar, D. Relyea, S. Rock, O. Saxton, Z. Szalata, J. Turner, and M. Woods, “Helicity-correlated systematics for SLAC experiment E158,” *IEEE Trans. Nucl. Sci.* **49**, 1097–1105 (2002).
4. Q weak collaboration, D. Androic, D. S. Armstrong, A. Asaturyan, T. Averett, J. Balewski, J. Beaufait, R. S. Beminiwatha, J. Benesch, F. Benmokhtar, J. Birchall, R. D. Carlini, G. D. Cates, J. C. Cornejo, S. Covrig, M. M. Dalton, C. A. Davis, W. Deconinck, J. Diefenbach, J. F. Dowd, J. A. Dunne, D. Dutta, W. S. Duvall, M. Elaasar, W. R. Falk, J. M. Finn, T. Forest, D. Gaskell, M. T. W. Gericke, J. Grames, V. M. Gray, K. Grimm, F. Guo, J. R. Hoskins, K. Johnston, D. Jones, M. Jones, R. Jones, M. Kargiantoulakis, P. M. King, E. Korkmaz, S. Kowalski, J. Leacock, J. Leckey, A. R. Lee, J. H. Lee, L. Lee, S. MacEwan, D. Mack, J. A. Magee, R. Mahurin, J. Mammei, J. W. Martin, M. J. McHugh, D. Meekins, J. Mei, R. Michaels, A. Micherdzinska, A. Mkrtchyan, H. Mkrtchyan, N. Morgan, K. E. Myers, A. Narayan, L. Z. Ndukum, V. Nelyubin, Nuruzzaman, W. T. H. van Oers, A. K. Opper, S. A. Page, J. Pan, K. D. Paschke, S. K. Phillips, M. L. Pitt, M. Poelker, J. F. Rajotte, W. D. Ramsay, J. Roche, B. Sawatzky, T. Seva, M. H. Shabestari, R. Silwal, N. Simicevic, G. R. Smith, P. Solvignon, D. T. Spayde, A. Subedi, R. Subedi, R. Suleiman, V. Tadevosyan, W. A. Tobias, V. Tvaskis, B. Waidyawansa, P. Wang, S. P. Wells, S. A. Wood, S. Yang, R. D. Young, and S. Zhamkochyan, “First determination of the weak charge of the proton,” *Phys. Rev. Lett.* **111**, 141803 (2013).
5. B. Santos, S. Gallego, A. Mascaraque, K. F. McCarty, A. Quesada, A. T. N’Diaye, A. K. Schmid, and J. de la Figuera, “Hydrogen-induced reversible spin-reorientation transition and magnetic stripe domain phase in bilayer Co on Ru (0001),” *Phys. Rev. B* **85**, 134409 (2012) and references therein.
6. S. Mayer and J. Kessler, “Experimental verification of electron optic dichroism,” *Phys. Rev. Lett.* **74**, 4803–4806 (1995).
7. K. W. Trantham, M. E. Johnston, and T. J. Gay, “Failure to observe electron circular dichroism in camphor,” *J. Phys. B* **28**, L543–L548 (1995).

8. J. M. Dreiling and T. J. Gay, "Chirally sensitive electron-induced molecular breakup and the Vester-Ulbricht hypothesis," *Phys. Rev. Lett.* **113**, 118103 (2014).
9. T. J. Gay, "Physics and technology of polarized electron scattering from atoms and molecules," in *Advances in Atomic, Molecular, and Optical Physics*, E. Arimondo, P. R. Berman, and C. C. Lin, eds. (Academic, 2009), Vol. **57**, pp.157–247.
10. T. J. Gay and F. B. Dunning, "Mott electron polarimetry," *Rev. Sci. Instrum.* **63**, 1635–1651 (1992).
11. J. M. Dreiling, "Asymmetric interactions between spin-polarized electrons and chiral molecules," Ph.D. dissertation (University of Nebraska, 2014).
12. M. I. Fabrikant, K. W. Trantham, V. M. Andrianarijaona, and T. J. Gay, "Active feedback scheme for minimization of helicity-dependent instrumental asymmetries," *Appl. Opt.* **47**, 2465–2469 (2008).
13. G. D. Cates, University of Virginia, Charlottesville, Virginia (personal communication, 2014).